

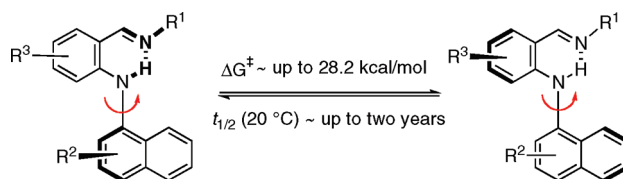
Insights into the Origins of Configurational Stability of Axially Chiral Biaryl Amines with an Intramolecular N–H–N Hydrogen Bond

Kazuhiro Hayashi, Nobuyuki Matubayasi, Changsheng Jiang, Tomoyuki Yoshimura, Swapan Majumdar, Takahiro Sasamori, Norihiro Tokitoh, and Takeo Kawabata*

Institute for Chemical Research, Kyoto University, Uji, Kyoto 611-0011, Japan

kawabata@scl.kyoto-u.ac.jp

Received April 1, 2010



Configurationally stable chiral biaryl amines with an intramolecular N–H–N hydrogen bond have been developed. The barriers for racemization are in the range of 19.3–28.2 kcal/mol, which corresponds to the half-lives of racemization of the enantiomers in the range of 7 s to 2 years at 20 °C. Enantiomers of some of these compounds were separable by HPLC with chiral stationary phases. The biaryl amines are supposed to have a conformation similar to that of a binaphthyl skeleton, which was indicated by an X-ray crystal analysis of a biaryl amine. The N–H appears at 11.1–13.3 ppm in their ¹H NMR spectrum in CDCl₃, indicating strong hydrogen bonding. Biaryl amines with an extremely strong intramolecular N–H–N hydrogen bond ($\delta_{\text{NH}} \sim 13$ ppm) were assumed to undergo racemization without cleavage of an N–H–N hydrogen bond, while those with a mediumly strong N–H–N hydrogen bond ($\delta_{\text{NH}} \sim 11$ ppm) are assumed to undergo racemization via cleavage of an N–H–N hydrogen bond. Hydrogen/deuterium exchange of a chiral biaryl amine was found to proceed without any trace of racemization.

Introduction

Chiral binaphthyls have been extensively used in asymmetric synthesis. In particular, metal complexes of 2,2'-disubstituted 1,1'-binaphthyls (**1**) have been shown to be extremely effective catalysts for a variety of asymmetric transformations (Figure 1).^{1–3} While the catalytically active metal center (M) in **1** is separated from the chiral axis (C(1)–C(1')) by three bonds, it is quite effective for asymmetric induction in many cases. The ultimate structure to minimize the distance between the catalytically active metal center and the chiral axis is shown as **2**, where the central metal is directly connected to the chiral C(1')–X axis. Rational precursors for **2** are shown as **3**.

A crucial question about **3** was whether enantiomers of **3** with axial chirality could exist without rapid racemization at ambient temperature. We have reported that several chiral biaryl amines with an intramolecular N–H–N hydrogen bond such as **3** are tolerant against racemization at ambient temperature and have racemization barriers up to 28.2 kcal/mol,

which corresponds to a half-life of racemization of 24 months at 20 °C.⁴ An extremely strong hydrogen bond was assumed to be the key to maintain the enantiomeric stability of the biaryl amines. We describe here the properties of axially chiral biaryl amines with an intramolecular N–H–N hydrogen bond and the possible origins of their exceptional tolerance against racemization.^{5–7}

(4) Kawabata, T.; Jiang, C.; Hayashi, K.; Tsubaki, K.; Yoshimura, T.; Majumdar, S.; Sasamori, T.; Tokitoh, N. *J. Am. Chem. Soc.* **2009**, *131*, 54–55.

(5) Conformationally stable atropisomers of biaryl ethers have been reported; see: (a) Fuji, K.; Oka, T.; Kawabata, T.; Kinoshita, T. *Tetrahedron Lett.* **1998**, *39*, 1373–1376. (b) Betson, M. S.; Clayden, J.; Worrall, C. P.; Peace, S. *Angew. Chem., Int. Ed.* **2006**, *45*, 5803–5807. (c) Clayden, J.; Worrall, C. P.; Moran, W. J.; Helliwell, M. *Angew. Chem., Int. Ed.* **2008**, *47*, 3234–3237.

(6) For an example of conformational studies of alkyl aryl amines, see: Casarini, D.; Lunazzi, L.; Placucci, G. *J. Org. Chem.* **1987**, *52*, 4721–4726.

(7) For asymmetric synthesis of atropisomeric aromatic amine derivatives, see: (a) Curran, D. P.; Qi, H.; Geib, S. J.; DeMello, N. C. *J. Am. Chem. Soc.* **1994**, *116*, 3131–3132. (b) Hughes, A. D.; Simpkins, N. S. *Synlett* **1998**, 967–968. (c) Ates, A.; Curran, D. P. *J. Am. Chem. Soc.* **2001**, *123*, 5130–5131. (d) Clayden, J.; Mitjans, D.; Youssef, L. H. *J. Am. Chem. Soc.* **2002**, *124*, 5266–5267. (e) Kitagawa, O.; Yoshikawa, M.; Tanabe, H.; Morita, T.; Takahashi, M.; Dobashi, Y.; Taguchi, T. *J. Am. Chem. Soc.* **2006**, *128*, 12923–12931. (f) Brandes, S.; Bella, M.; Kjarsgaard, A.; Jørgensen, K. A. *Angew. Chem., Int. Ed.* **2006**, *45*, 1147–1151. (g) Leusse, S. B.; Counciller, C. M.; Wilt, J. C.; Perkins, B. R.; Johnston, J. N. *Org. Lett.* **2008**, *10*, 2445–2447.

(1) Mei, L.; Xuan, L. X. *Asian J. Chem.* **2006**, *18*, 2089–2106.

(2) Brunel, J. M. *Chem. Rev.* **2005**, *105*, 857–897.

(3) Kocovsky, P.; Vyskocil, S.; Smrcina, M. *Chem. Rev.* **2003**, *103*, 3213–3245.

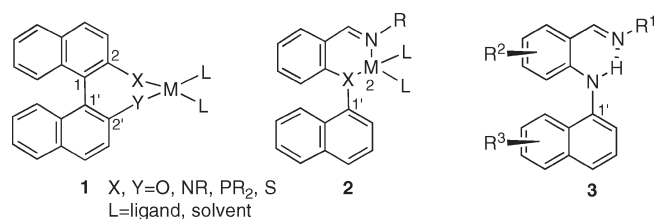
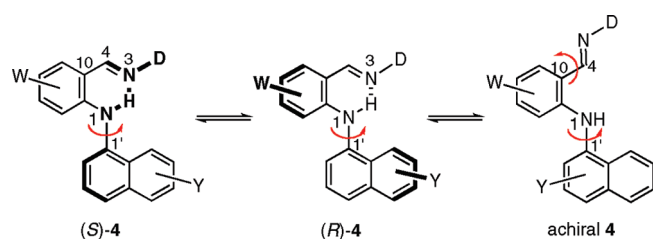


FIGURE 1. Central metal (M) is directly connected to the chiral C(1')–X axis in binaphthyl surrogates **2**, while M in **1** is separated from the chiral axis (C(1')–C(1'')) by three bonds. Biaryl amines **3** are possible precursors to **2**.

SCHEME 1. Hypothetical Scheme for Configurationally Stable Axially Chiral Biaryl Amines with an Intramolecular N–H–N Hydrogen Bond



Results and Discussion

A hypothetical scheme for the design of configurationally stable axially chiral biaryl amines **4** is shown in Scheme 1. One of the critical preconditions for **4** is the formation of an extremely strong hydrogen bond, since the non-hydrogen-bonded form of **4** must adopt an *s-trans* conformation around the C(4)–C(10) bond and it should be achiral due to rapid bond rotation around the C(1')–N(1) axis. To generate a stronger hydrogen bond, donor substituents **D** on N(3) and electron-withdrawing substituents **W** on the upper pseudonaphthalene ring are assumed to be preferable. Sterically demanding substituents **Y** on the lower naphthalene ring are expected to be effective in increasing the rotational barrier around the C(1')–N(1) axis.

Several biaryl amines **5–11** were prepared via Buchwald cross-coupling reactions⁸ between substituted 1-aminonaphthalenes and substituted phenyl bromides (Figure 2). Chiral properties of these amines were investigated (Table 1).⁴ The rotational barrier of the N(1)–C(1') bond of **5** was determined to be 19.3 kcal/mol (92 °C) by variable-temperature NMR measurements in toluene-*d*₈ (400 MHz NMR, $\Delta\nu_{AB}$ = 9.9 Hz, T_{coales} = 365 K, entry 1). The half-life of racemization of **5** at 20 °C was estimated to be ca. 7 s based on the activation entropy (–5.0 eu, vide infra). Enantiomers of **6–12** could be separated at ambient temperature by HPLC with chiral stationary phases. The processes for time-dependent racemization of the separated enantiomers were monitored by HPLC analysis at 22 °C for **6–8** and at 80 °C for **9–12**, and their racemization barriers are shown in entries 2–8 in Table 1. The half-lives of racemization of **9–12** at 20 °C were roughly estimated on the assumption that ΔS^\ddagger of the restricted C–N bond rotation is nearly zero. The ¹H NMR chemical shifts of N–H of compounds **9–12** in CDCl₃ are in

the range of δ 13.01–13.33 ppm, which indicates the extremely strong hydrogen bonding. This observation is consistent with the hypothesis that strong hydrogen bonding is critical for configurationally stable axial chirality. Substituent effects at N(3) were investigated with compounds **9–12** (entries 5–8). The half-life of racemization increased with an increase in the donating ability of the substituents among these compounds. The contribution of the electron-withdrawing group (NO₂) to the configurational stability of axial chirality is obvious when the half-life of racemization of **10** with 6,8-dinitro substituents (4.3 months) is compared with that of **8** with 6,8-dimethyl substituents (2.4 days) (entries 4 vs 6). The larger rotational barrier of **10** compared to that of **8** does not seem to be due to steric effects because the steric bulkiness of a nitro group (*A* value = ~1.2) is estimated to be similar or even smaller than that of a methyl group (*A* value = ~1.7). On the other hand, steric effects on the naphthalene ring are obvious when the half-life of racemization of **6** (2.3 h) is compared with that of **12** (24 months), which has an additional 8'-methyl substituent (entries 2 vs 8). Among these compounds, compound **12** with an electron-donating isopropyl group at N(3), electron-withdrawing nitro groups at C(6) and C(8), and sterically demanding methyl groups at C(2') and C(8') has the largest rotational barrier and the longest half-life of racemization (entry 8). The observation is consistent with the hypothesis for the design of axially chiral biaryl amines with high configurational stability shown in Scheme 1.

An X-ray structure of a single crystal of **11** is shown in Figure 3.⁴ A ring consisting of nine atoms of N(1)–C(9)–C(8)–C(7)–C(6)–C(5)–C(10)–C(4)–N(3) is almost completely planar (Figure 3, a and b), which suggests the formation of a pseudonaphthalene ring involving the N–H–N hydrogen bond. The dihedral angle between the pseudonaphthalene ring and the naphthalene ring is 128° (Figure 3, b). The CD spectra of the separated enantiomers of **11** clearly indicate the enantiomeric relationship.⁴ All of the experimental evidence indicates the biaryl amine **11** has a conformation similar to that of binaphthyl skeletons. The observed distance (2.67 Å) between N(3) and N(1) of **11** indicates the strong hydrogen bonding, which is comparable to the reported distance (2.69 Å) of the intramolecular N–H–N hydrogen bond of the related anilido aldimine derivative⁹ and is much shorter than the intermolecular counterpart (2.92 Å).¹⁰

We next investigated the mechanistic aspects on racemization of these chiral biaryl amines. We had anticipated that an intramolecular N–H–N hydrogen bond is critical for the configurational stability of the axially chiral biaryl amines, since the non-hydrogen-bonded form of **4** must adopt an *s-trans* conformation around the C(4)–C(10) bond and it should be readily racemized due to rapid bond rotation around the C(1')–N(1) axis. This assumption was confirmed by the properties of compound **13**, the corresponding *N*-methyl derivative of **5** (Figure 4). The NOESY spectrum of **13** indicates its *s-trans* conformation around the C(4)–C(10) bond. The rotational barrier of the N(1)–C(1') bond was determined to be 15.6 kcal/mol (54 °C) by variable-temperature NMR measurements in toluene-*d*₈ (400 MHz NMR, $\Delta\nu_{AB}$ = 123.8 Hz,

(8) Wolfe, J. P.; Wagaw, S.; Buchwald, S. L. *J. Am. Chem. Soc.* **1996**, *118*, 7215–7216.

(9) Lee, B. Y.; Kwon, H. Y.; Lee, S. Y.; Na, S. J.; Han, S.-i.; Yun, H.; Lee, H.; Park, Y.-W. *J. Am. Chem. Soc.* **2005**, *127*, 3031–3037.

(10) Brennan, C. J.; McKee, V. *Acta Crystallogr.* **1999**, *C55*, 1492–1494.

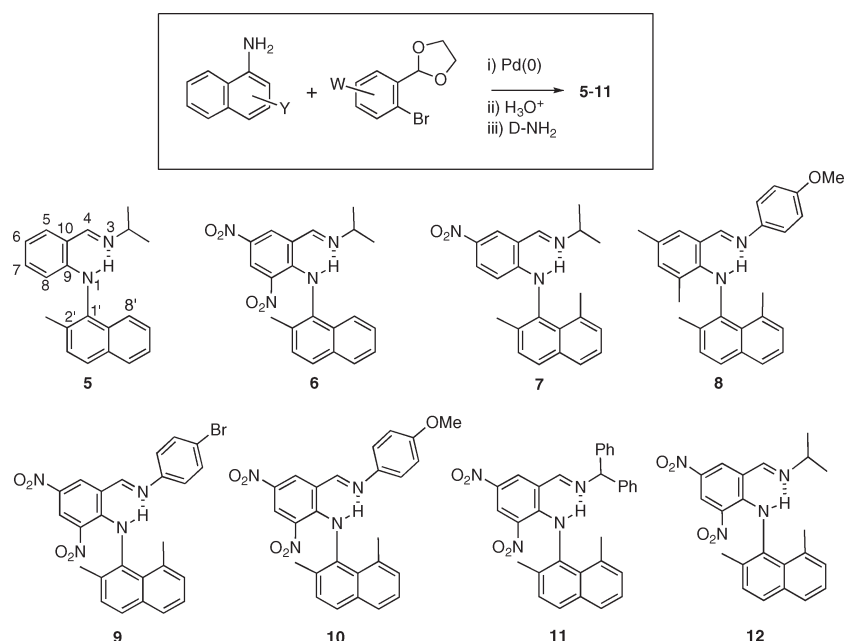


FIGURE 2. Preparation and structures of biaryl amines 5–12.

TABLE 1. Behavior toward Racemization of Biaryl Amines with an Intramolecular N–H–N Hydrogen Bond

entry	compd	$\Delta G^{\ddagger a}$ (kcal/mol)	$t_{1/2}$ (racemization) (20 °C)	δ_{NH}^b (ppm)
1	5	19.3 (92 °C) ^c	7 s ^d	11.07
2	6	23.2 (22 °C) ^e	2.3 h ^f	13.47
3	7	23.6 (22 °C) ^e	5.0 h ^f	12.02
4	8	24.9 (22 °C) ^e	2.4 days ^f	11.44
5	9	27.0 (80 °C) ^g	3.0 months ^h	13.01
6	10	27.2 (80 °C) ^g	4.3 months ^h	13.33
7	11	27.4 (80 °C) ^g	6.0 months ^h	13.24
8	12	28.2 (80 °C) ^g	24 months ^h	13.30

^aRotational barrier of the chiral axis at the temperature indicated in parentheses. ^b¹H NMR (400 MHz) chemical shift (ppm) of N–H measured in CDCl₃ at 21 °C. ^cDetermined by VNMR. ^dDetermined on the basis of $\Delta S^{\ddagger} = -5.0$ eu (see Table 2, entry 1). ^eDetermined by time-dependent racemization of an isolated enantiomer at 22 °C by HPLC analysis. ^fHalf-life or racemization at 22 °C determined by time-dependent racemization of an isolated enantiomer by HPLC analysis. ^gDetermined by time-dependent racemization of an isolated enantiomer at 80 °C (benzene reflux) by HPLC analysis. ^hHalf-life of racemization at 20 °C roughly estimated on the assumption that ΔS^{\ddagger} of the restricted C–N bond rotation is nearly zero.

$T_{\text{coales}} = 327$ K), which was much smaller than that of **5** (19.3 kcal/mol). The larger rotational barrier of **5** than **13** would be attributed to the difference in the preferred conformation of **5** from that of **13** (i.e., *s-cis* conformation for **5** and *s-trans* conformation for **13**) because **5** should have a smaller rotational barrier than **13** due to the fewer substituents on N(1) if both of them could adopt the *s-trans* conformation (Figure 4).

The strength of the intramolecular N–H–N hydrogen bond of the biaryl amines appears to be critically related to the racemization barriers of the biaryl amines. An increase in the strength of the hydrogen bond by the electron-withdrawing NO₂ groups at C(6) and C(8) in **10** is assumed to be the origin of its larger racemization barrier (27.2 kcal/mol) than that of **8** (24.9 kcal/mol) possessing the corresponding methyl groups. The racemization barriers of compounds **9–12** increased with an increase in the donating ability of the substituents at

N(3), probably due to the increase in the strength of the hydrogen bond (Table 1, entries 5–8). On the basis of this data, two hypothetical mechanisms for the racemization of the biaryl amines are shown in Scheme 2. The first one involves direct bond rotation of the N(1)–C(1') chiral axis without cleavage of an N–H–N hydrogen bond (a). The second one involves *s-cis/s-trans* isomerization through the C(10)–C(4) bond rotation with concomitant cleavage of an N–H–N hydrogen bond (b). We envisaged relatively small solvent effects for the racemization process via the former mechanism. The racemization barrier is expected to be less solvent-dependent, and the entropy term is to be less significant. Actually, activation entropies in the range of -5.2 to -9.9 eu for the racemization process of 1,1'-binaphthyl derivatives have been reported.¹¹ On the other hand, relatively large solvent effects on the racemization barrier and the large negative activation entropy are expected for the racemization process via the latter mechanism because the NH-free intermediate with an *s-trans* configuration is expected to undergo solvation more significantly than the corresponding *s-cis* congener. Polar solvents may be expected to decrease the racemization barrier due to stabilization of this intermediate.

The barriers and the activation entropies for the racemization process of **5** in various solvents were determined (Table 2). The ¹H NMR spectrum of **5** at 20 °C showed two diastereotopic isopropyl methyl peaks, indicating restricted bond rotation along the C(1')–N(1) axis. The rotational barriers of the N(1)–C(1') bond (the racemization barriers of the biaryl amines) at the coalescence temperature in each solvent were shown in entries 1–7. The activation entropies (ΔS^{\ddagger}) for the racemization process were determined from temperature dependence of the racemization barriers, which were obtained by line shape analyses of ¹H NMR signals of the isopropyl methyl peaks (see the Supporting Information).

(11) (a) Badar, Y.; Cooke, A. S.; Harris, M. M. *J. Chem. Soc.* **1965**, 1412–1418. (b) Colter, A. K.; Clemens, L. M. *J. Am. Chem. Soc.* **1965**, *87*, 847–852.

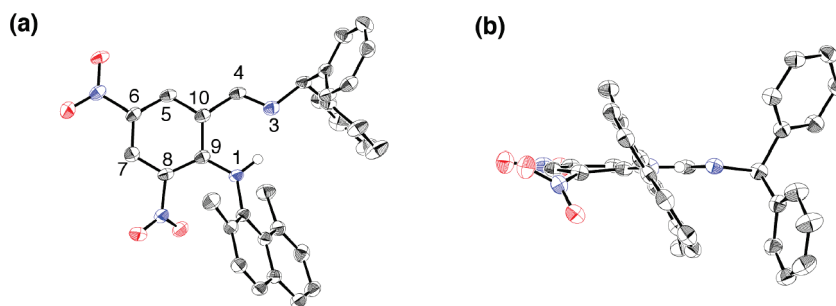


FIGURE 3. X-ray structure of **11**: (a) top view; (b) side view. Displacement ellipsoids were drawn at the 50% probability level. Hydrogens except N–H were omitted for clarity.

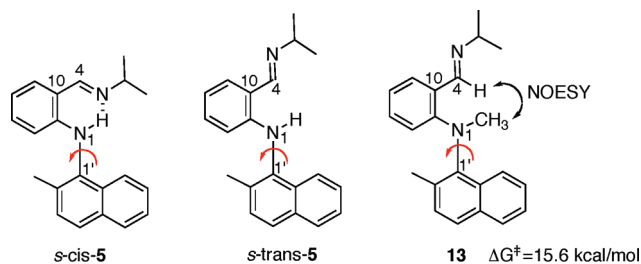
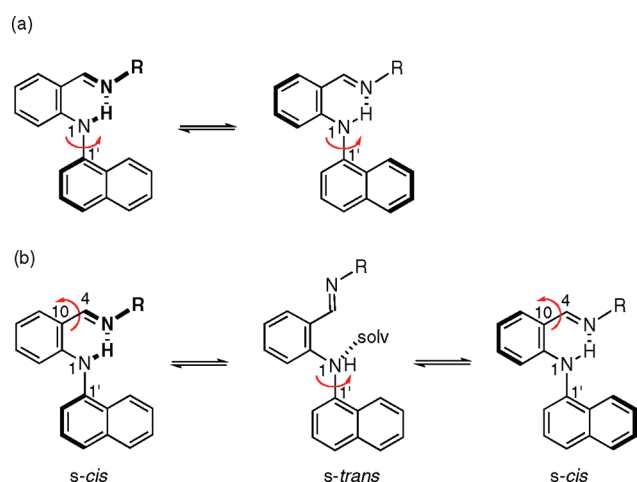


FIGURE 4. *s-cis*- and *s-trans*-conformers of **5**, *s-trans*-conformer of **13**, and the rotational barrier around the N(1)–C(1') bond of **13**.

SCHEME 2. Possible Mechanisms for Racemization of Biaryl Amines (a) via Direct Rotation of the Chiral N(1)–C(1') Axis and (b) via *s-cis*/*s-trans* Isomerization through the C(10)–C(4) Bond Rotation



In more polar solvents such as ethanol-*d*₆, DMF-*d*₇, and acetonitrile-*d*₃, smaller racemization barriers (17.8–18.0 kcal/mol) were observed (entries 5–7), while larger racemization barriers (18.9–19.3 kcal/mol) were observed in less polar solvents such as toluene-*d*₈ and (CDCl₂)₂ (entries 1 and 2). Large negative activation entropies (–18 to –25 eu) were observed for the racemization process especially in polar solvents (entries 5–7). The observation indicates that racemization of **5** might proceed, especially in polar solvents, through the mechanism via *s-cis*/*s-trans* isomerization as shown in Scheme 2 (b). However, it is totally unclear whether racemization of **5** in less polar solvents such as toluene-*d*₈ proceeds via the same mechanism because activation entropies

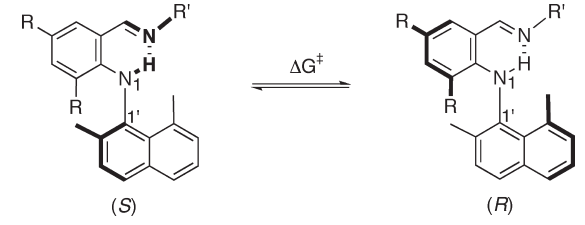
TABLE 2. Activation Parameters for the Racemization Process of **5** in Various Solvents

entry	solvent	ϵ^a	$\Delta G^{\ddagger b,c}$ (kcal/mol)	$\Delta S^{\ddagger d}$ (eu)
1	toluene- <i>d</i> ₈	2.6	19.3 (92 °C), [9.9]	–5.0
2	(CDCl ₂) ₂	8.2	18.9 (86 °C), [10.7]	–15
3	pyridine- <i>d</i> ₅	12.3	18.4 (81 °C), [14.8]	<i>e</i>
4	isopropanol- <i>d</i> ₈	18.3	18.3 (74 °C), [9.2]	–15
5	ethanol- <i>d</i> ₆	24.6	17.9 (66 °C), [9.0]	–18
6	DMF- <i>d</i> ₇	36.7	17.8 (64 °C), [7.8]	–25
7	acetonitrile- <i>d</i> ₃	37.5	18.0 (67 °C), [9.0]	–18

^aDielectric constant of the undeuterated solvents quoted from *Lange's Handbook of Chemistry*, 13th ed; Dean, J. A., Ed.; McGraw Hill: New York, 1972. ^bRotational barrier of the chiral axis at the temperature indicated in parentheses. ^cDetermined from $\Delta\nu$ (Hz) indicated in brackets and the coalescence temperature obtained by V NMR. ^dDetermined from temperature dependency of the racemization barriers; see the Supporting Information. ^eNot determined.

for the racemization process were much smaller in magnitude (entry 1, –5.0 eu).

We next examined the racemization processes of **8** and **11**. Racemization barriers of **8** were determined by time-dependent racemization of the isolated enantiomer in various solvents at 20 °C and are shown in entries 1–4 of Table 3. The barriers in benzene, toluene, ethanol, and DMF are 24.9, 25.2, 23.7, and 23.8 kcal/mol, respectively. The activation entropy for the racemization process of **8** in DMF was determined to be 20 eu from racemization barriers of **8** at –6 °C (23.1 kcal/mol), 9 °C (23.4 kcal/mol), 17 °C (23.6 kcal/mol), 31 °C (23.8 kcal/mol), and 42 °C (24.0 kcal/mol), which were also determined by time-dependent racemization of the isolated enantiomer of **8** at the indicated temperature (see the Supporting Information). The racemization barriers of **8** were solvent-dependent and were smaller in more polar solvents. A large negative activation entropy (–20 eu) was observed for the racemization process of **8** in DMF (entry 4). The observation also indicates that racemization of **8** might proceed through the mechanism via *s-cis*/*s-trans* isomerization as shown in Scheme 2 (b). Similarly, racemization barriers of **11** were determined by time-dependent racemization of the isolated enantiomer in various solvents at 78–83 °C and are shown in entries 5–8 of

TABLE 3. Activation Parameters for the Racemization Processes of **8 and **11** in Various Solvents**


entry	R	compd	solvent	$\Delta G^{\ddagger a}$ (kcal/mol)	$\Delta S^{\ddagger b}$ (eu)
1	Me	8	benzene	24.9 (20 °C)	<i>c</i>
2	Me	8	toluene	25.2 (20 °C)	<i>c</i>
3	Me	8	ethanol	23.7 (20 °C)	<i>c</i>
4	Me	8	DMF	23.8 (20 °C)	-20
5	NO ₂	11	benzene	27.4 (80 °C)	<i>c</i>
6	NO ₂	11	toluene	27.5 (83 °C)	<i>c</i>
7	NO ₂	11	ethanol	27.9 (78 °C)	<i>c</i>
8	NO ₂	11	DMF	28.1 (80 °C)	-2.0

^aDetermined by time-dependent racemization of the isolated enantiomer at the temperature indicated in parentheses. ^bDetermined from temperature-dependent racemization barriers; see the Supporting Information. ^cNot determined.

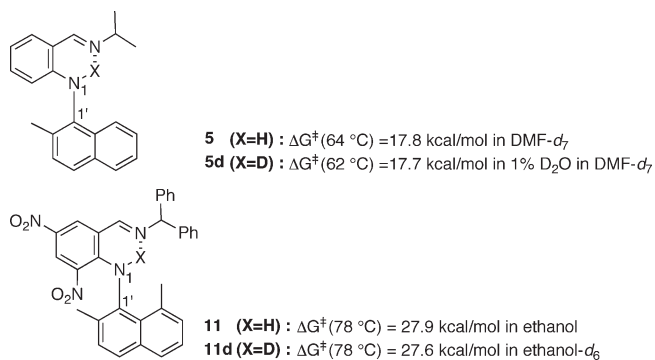
**FIGURE 5.** Comparison of the racemization barriers of **5** and **11** with those of their deuterated derivatives **5d** and **11d**, respectively.

Table 3. Contrary to the cases of **5** and **8**, solvent dependency of the racemization barriers of **11** was less significant, and the barrier in DMF was slightly larger than that in benzene. Activation entropy for the racemization process in DMF was close to zero (-2.0 eu, entry 8). The observation indicates that racemization of **11** might proceed through the mechanism via direct rotation of the N(1)-C(1') chiral axis without cleavage of an N-H-N hydrogen bond as shown in Scheme 2 (a). On the basis of these results, it would be assumed that biaryl amines with an extremely strong intramolecular N-H-N hydrogen bond such as **9-12** undergo racemization without cleavage of an N-H-N hydrogen bond and, thus, are tolerant against racemization. On the other hand, biaryl amines with a mediumly strong N-H-N hydrogen bond such as **5** and **8** are assumed to undergo racemization via cleavage of an N-H-N hydrogen bond.

We then investigated the deuterium isotope effect on the N-H-N hydrogen bonding. Scheiner and Čuma reported that deuterium bonding between D₂O (DO-D...OD₂) was estimated to be stronger than hydrogen bonding between H₂O (HO-H...OH₂) by ~0.5 kcal/mol by ab initio

calculations.¹² We were interested in the deuterium isotope effect on the racemization behavior of the chiral biaryl amines. The NH signal of **5** appeared at δ 11.3 ppm in ¹H NMR in DMF-*d*₇ disappeared immediately after the addition 1% D₂O, indicating the formation of **5d** (Figure 5). The rotational barrier around the N(1)-C(1') axis of **5d** was determined by variable-temperature NMR to be 17.7 kcal/mol at 62 °C. Essentially no deuterium effect on the rotational barrier of **5** was observed. Next, the racemization barrier of **11d** was measured by time-dependent racemization of enantio-enriched **11d** in ethanol-*d*₆ at 78 °C.¹³ Enantioenriched **11d** was prepared by hydrogen/deuterium exchange of **11** (84% ee) without loss of enantiomeric purity (vide infra). Racemization barrier of **11d** (27.6 kcal/mol) was comparable to that of **11**. The observation indicates that deuterium effects on the rotational barriers of these biaryl amines were not significant, irrespective of the mechanism of the racemization.

We finally examined whether racemization of **11** takes place on hydrogen/deuterium exchange process of the N-H-N group (Scheme 3). After formation of **11d** by treatment of **11** (95% ee) with 1% D₂O in DMF-*d*₇ at 20 °C for 1 h, **11d** was treated with brine to give **11** back, whose ee was found to be 95% ee. No racemization took place during the hydrogen/deuterium exchange process. This might indicate that hydrogen/deuterium exchange proceeds via an ammonium intermediate without an N-H(D)-N bond cleavage. The observed property of **11** may be beneficial when enantiomerically enriched organometallic species such as **2** are to be prepared from enantiomerically enriched precursor **3** because the hydrogen/metal exchange process may proceed in the similar way to the hydrogen-deuterium exchange process depending on the nature of metal sources.¹⁴

Conclusions

We have developed chiral biaryl amines with an intramolecular N-H-N hydrogen bond which possess configurationally stable axial chirality at ambient temperature. The half-lives of racemization of the chiral biaryl amines are up to 2 years at 20 °C. These biaryl amines are supposed to have a conformation similar to that of 1,1'-binaphthyl derivatives, which was indicated by an X-ray crystal analysis of **11**. Biaryl amines with an extremely strong intramolecular N-H-N hydrogen bond such as **9-12** were assumed to undergo racemization without cleavage of an N-H-N hydrogen bond, while those with a mediumly strong N-H-N hydrogen bond such as **5** and **8** are assumed to undergo racemization mostly via cleavage of an N-H-N hydrogen bond. Hydrogen/deuterium exchange of **11** was found to proceed without any trace of racemization.

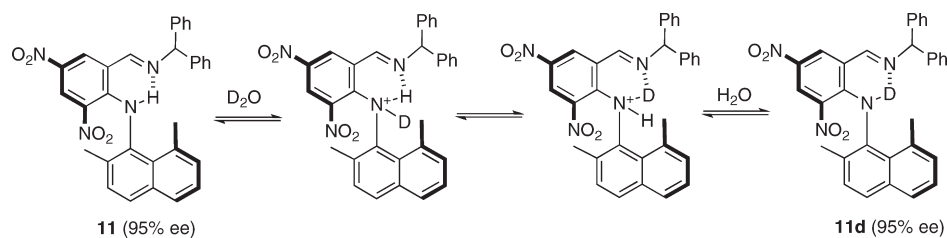
Experimental Section

Compounds 5-12. Preparation and spectroscopic data of compounds **5-12** were reported in the Supporting Information of our previous publication: see ref 4.

(13) Compound **11d** was prepared by addition of D₂O to a DMF-*d*₇ solution of **11**, and its formation was confirmed by disappearance of the NH signal at δ 13.6 ppm in the ¹H NMR in DMF-*d*₇. After removal of the solvents under vacuum at ambient temperature, the residue was dissolved in ethanol-*d*₆ for measurement of the racemization barrier.

(14) Recently, we have prepared an anilidoaldimine aluminum complex from **5** and found that the racemization barrier of the aluminum complex was higher by ca. 4 kcal/mol than the corresponding biaryl amine precursor with an N-H-N hydrogen bond; see: Hayashi, K.; Nakajima, Y.; Ozawa, F.; Kawabata, K. *Chem. Lett.* **2010**, *39*, 643-645.

(12) Scheiner, S.; Čuma, M. *J. Am. Chem. Soc.* **1996**, *118*, 1511-1521.

SCHEME 3. Hydrogen/Deuterium Exchange of **11** without Racemization

(*E*)-*N*-(2-((isopropylimino)methyl)phenyl)-*N*,2-dimethylnaphthalen-1-amine (**13**). Iodomethane (3.0 mL, 48.2 mmol) was added to a stirred suspension of 2-methylnaphthalen-1-amine (7.45 g, 47.4 mmol) and K_2CO_3 (13.0 g, 94.3 mmol) in acetone (189 mL) at 0 °C. The mixture was heated under reflux of acetone for 10 h. After the mixture was cooled to room temperature, the solvent was removed in vacuo. The residue was purified by column chromatography (SiO₂, ethyl acetate/hexane = 1:8) to give 2-methyl-1-methylaminonaphthalene (3.22 g, 40% yield) as an oil: ¹H NMR (400 MHz, CDCl₃) δ 8.12 (d, *J* = 8.2 Hz, 1H), 7.81 (d, *J* = 7.8 Hz, 1H), 7.53–7.38 (m, 3H), 7.31 (d, *J* = 8.3 Hz, 1H), 3.32 (br s, 1H), 2.96 (s, 3H), 2.48 (s, 3H); ¹³C NMR (100 MHz, CDCl₃) δ 143.9, 133.5, 129.3, 128.4, 128.3, 125.3, 125.2, 124.8, 122.7, 122.5, 36.9, 18.0; IR (neat) 2945, 1572, 1510, 1468, 1372, 806 cm⁻¹; MS *m/z* (rel intensity) 171 (M⁺, 100), 156 (80), 128(20), 115 (17), 58 (18); HRMS calcd for C₁₂H₁₃N 171, 1048, found 171.1053. Anal. Calcd for C₁₂H₁₃N: C, 84.17; H, 7.65; N, 8.18. Found: C, 84.07; H, 7.78; N, 8.21.

A mixture of Pd₂(dba)₃–CHCl₃ (10 mg, 0.0175 mmol), P(*t*-Bu)₃–HBF₄ (3.7 mg, 0.0125 mmol), sodium *tert*-butoxide (358 mg, 3.75 mmol), 1-bromo-2-(diethoxymethyl)benzene (774 mg, 2.99 mmol), 2-methyl-1-methylaminonaphthalene (514 mg, 3.0 mmol), and toluene (11.2 mL) was prepared in a round-bottom flask placed in a glovebox. After the septum-sealed flask was taken out of the glovebox, the mixture was stirred at 80 °C for 12 h. After being cooled to room temperature, the mixture was diluted with ethyl acetate and washed with saturated aq NaHCO₃ and brine, dried over anhydrous Na₂SO₄, filtered, and evaporated in vacuo. The residue was purified by column chromatography (SiO₂, ethyl acetate/hexane = 1:10) to give the mixture of *N*-(2-(diethoxymethyl)phenyl)-*N*,2-dimethylnaphthalen-1-amine and 2-(methyl(2-methylnaphthalen-1-yl)amino)benzaldehyde. The mixture was dissolved in 5% aq HCl (21 mL) and THF (21 mL). After the mixture was heated under THF reflux for 5 h, saturated aq NaHCO₃ solution was added to the mixture until pH 8. The resulting mixture was extracted with ethyl acetate, and the organic phase was washed with brine, dried over anhydrous Na₂SO₄, filtered, and evaporated in vacuo. The residue was purified by column chromatography (SiO₂, ethyl acetate/hexane = 1:10) to give 2-(methyl(2-methylnaphthalen-1-yl)amino)benzaldehyde (807 mg, 98% for 2 steps) as yellow needles: mp (hexane) 89–90 °C; ¹H NMR (400 MHz, DMSO-*d*₆, 20 °C) δ 9.16 (br s, 1H), 7.98–7.39 (m, 9H), 6.88 (t, *J* = 7.6 Hz, 2H), 3.34 (s, 3H), 2.09 (br s, 3H); ¹³C NMR (100 MHz, DMSO-*d*₆, 20 °C) δ 189.2, 151.8, 144.9, 134.7, 133.4, 131.8, 130.1, 129.7, 128.8, 128.5, 127.3, 127.2, 125.6, 123.7, 122.6, 118.2, 115.8, 40.1, 17.9; ¹H NMR (400 MHz, DMSO-*d*₆, 100 °C) δ 9.50 (br s, 1H), 7.94–7.85 (m, 2H), 7.80

(d, *J* = 8.8 Hz, 1H), 7.53–7.38 (m, 5H), 6.95–6.82 (m, 2H), 3.37 (s, 3H), 2.15 (s, 3H); ¹³C NMR (100 MHz, DMSO-*d*₆, 100 °C) δ 188.7, 151.0, 142.7, 133.8, 133.1, 132.2, 129.9, 129.8, 129.1, 128.0, 126.7, 126.6, 125.0, 123.6, 122.1, 117.4, 115.6, 41.4, 17.2; IR (KBr) 2855, 1675, 1597, 1481, 1189, 816 cm⁻¹; MS *m/z* (rel intensity) 275 (M⁺, 100), 258 (42), 230 (30), 223 (25), 105 (40), 58 (61); HRMS calcd for C₁₉H₁₇NO 275.1310, found 275.1311. Anal. Calcd for C₁₉H₁₇NO: C, 82.88; H, 6.22; N, 5.09. Found: C, 83.07; H, 6.33; N, 5.04.

Isopropylamine (31 μL, 0.40 mmol) was added to a solution of 2-(methyl(2-methylnaphthalen-1-yl)amino)benzaldehyde (50 mg, 0.182 mmol) in toluene (5.0 mL). The mixture was heated under toluene reflux for 10 h. After the mixture was cooled to room temperature, the solvent was removed in vacuo to give **13** (57.5 mg, 100% yield) as a colorless oil: ¹H NMR (400 MHz, toluene-*d*₈, 20 °C) δ 8.02 (d, *J* = 8.3 Hz, 1H), 7.95 (d, *J* = 7.3 Hz, 1H), 7.74 (br s, 1H), 7.61 (d, *J* = 7.8 Hz, 1H), 7.40 (d, *J* = 8.7 Hz, 1H), 7.35–7.31 (m, 1H), 7.26–7.18 (m, 2H), 6.94 (d, *J* = 8.3 Hz, 1H), 6.82 (t, *J* = 7.3 Hz, 2H), 2.94 (s, 3H), 2.36 (br s, 1H), 1.80 (s, 3H), 0.81 (br s, 3H), 0.63 (br s, 3H); ¹³C NMR (100 MHz, toluene-*d*₈, 20 °C) δ 156.2, 150.2, 144.9, 134.2, 132.8, 132.0, 130.8, 130.2, 130.1, 128.6, 127.0, 126.5, 126.3, 125.4, 123.9, 119.6, 115.1, 61.2, 40.1, 24.0, 18.9; ¹H NMR (400 MHz, toluene-*d*₈, 90 °C) δ 7.99 (d, *J* = 8.2 Hz, 1H), 7.86 (dd, *J* = 7.8, 1.8 Hz, 1H), 7.77 (s, 1H), 7.60 (d, *J* = 8.2 Hz, 1H), 7.41 (d, *J* = 8.2 Hz, 1H), 7.31–7.24 (m, 1H), 7.23–7.11 (m, 2H), 6.98 (d, *J* = 8.7 Hz, 1H), 6.82 (d, *J* = 8.2 Hz, 1H), 6.77 (t, *J* = 7.8 Hz, 1H), 3.04 (s, 3H), 2.49 (sept, *J* = 6.0 Hz, 1H), 1.89 (s, 3H), 0.72 (d, *J* = 6.0 Hz, 6H); ¹³C NMR (100 MHz, toluene-*d*₈, 100 °C) δ 156.5, 150.3, 145.1, 134.7, 133.3, 132.5, 130.8, 130.7, 130.2, 128.8, 127.0, 126.94, 126.85, 125.6, 124.3, 119.8, 115.7, 60.8, 41.0, 23.9, 18.8; IR (neat) 2964, 1635, 1597, 1476, 1382, 753 cm⁻¹; MS (FAB) *m/z* (rel intensity) 339 (MNa⁺, 2), 317 (MH⁺, 100); HRMS (FAB⁺) calcd for C₂₂H₂₄N₂ 317.2018, found 317.2018.

Acknowledgment. We are grateful to Prof. Masaharu Nakamura, Kyoto University, for generous discussions on DFT calculations. This work was supported by a Grant-in-Aid for Exploratory Research from the Ministry of Education, Culture, Sports, Science and Technology, Japan, and by a Grant-in-Aid for JSPS Fellows to K.H.

Supporting Information Available: ¹H NMR and ¹³C NMR spectra. Determination of the activation parameters for the racemization processes. This material is available free of charge via the Internet at <http://pubs.acs.org>.